Band structure of charge-ordered doped antiferromagnets

Mats Granath*
Chalmers Technical University, Göteborg 41296, Sweden
(Received 21 January 2004; revised manuscript received 7 April 2004; published 30 June 2004)

We study the distribution of electronic spectral weight in a doped antiferromagnet with various types of charge order, and compare to angle resolved photoemission experiments on lightly doped $La_{2-x}Sr_xCuO_4$ (LSCO) and electron-doped $Nd_{2-x}Ce_xCuO_{4\pm\delta}$. Calculations on in-phase stripe and bubble phases for the electron-doped system are both in good agreement with the experiment, including, in particular, the existence of in-gap spectral weight. In addition we find that for in-phase stripes, in contrast to antiphase stripes, the chemical potential is likely to move with doping. For the hole-doped system we find that "staircase" stripes, which are globally diagonal but locally vertical or horizontal, can reproduce the photoemission data with the characteristic "Fermi arcs," whereas pure diagonal stripes cannot. We also calculate the magnetic structure factors of such staircase stripes and find that as the stripe separation is decreased with increased doping, these evolve from diagonal to vertical, separated by a coexistence region. The results suggest that the transition from horizontal to diagonal stripes seen in neutron scattering on underdoped LSCO may be a crossover between a regime where the typical length of straight stripe segments is longer than the interstripe spacing, to one where it is shorter and that, locally, the stripes are always aligned with the Cu-O bonds.

DOI: 10.1103/PhysRevB.69.214433 PACS number(s): 74.20.−z, 74.25.Jb, 74.72.−h

I. INTRODUCTION

In several families of superconducting cuprates there is evidence for *stripes*, which are regularly spaced quasi-one-dimensional structures where the doped charge congregates.[1] At the same time, there is a well-developed theory of high-temperature superconductivity in a system of weakly coupled Hubbard ladders.[2–4] It is thus quite natural to speculate that such a theory is, in fact, realized in the cuprates. One obvious objection to the stripe scenario of superconductivity is the lack of convincing evidence for the existence of stripes in several materials given that the strongest evidence is found in the relatively low-T_c $La_{2-x}Sr_xCuO_4$ (LSCO) family.[5] From a theoretical point of view, the lack of direct evidence is not immediately discouraging because stripe order is bad for superconductivity, whereas more elusive dynamic charge stripe correlations are good.[6,7] However, even in a system such as LSCO where stripes are well established, there are still issues about their fundamental implications on the electron dynamics. In particular, it seems that the distribution of low-energy spectral weight in k space as probed by angle-resolved photoemission spectroscopy (ARPES) does not show any clear evidence of the suggested quasi-one-dimensional (1D) nature of the electronic states, looking instead like the Fermi surface of a fully two-dimensional (2D) system.[8] On the other hand, ARPES also provides clear evidence of exotic physics, perhaps electron fractionalization,[9] with spectral functions that are typically very broad in energy and not consistent with a Fermi liquid-based quasiparticle description.[10]

A simple model for studying the distribution of single electron spectral weight in a charge-ordered doped antiferromagnet was introduced by Salkola *et al.*[11] in which all the complicated physics, which is responsible for the stripe formation and integrity, is replaced by a hand-picked potential which emulates the local environment of electrons in a stripe-ordered antiferromagnet. The potential is simply a staggered field representing the local antiferromagnetism, together with antiphase domain walls of suppressed field strength representing stripes. The spacings of the stripes are chosen in such a way that the model by construction will reproduce the diffraction response of a stripe-ordered system. The stripe placements are static but may be chosen in an irregular fashion, simulating quenched disorder or dynamic stripes which are fluctuating slowly compared to time scales of the local electron dynamics. Using this model for a disordered array of quarter-filled "bond-aligned"[12] stripes, it was found that the low-energy spectral weight forms a two-dimensional Fermi surface with, in particular, spectral weight in the "nodal regions," near $(\pi/2,\pi/2)$, which naively corresponds to propagation diagonally with respect to the stripe direction. A more detailed study of this model was carried out in Ref. 13 where it was realized that even a single stripe with one-dimensional states localized transverse to the stripe captures the qualitative features of the low-energy spectral weight as seen in ARPES in the under- and optimally doped LSCO with the full spectral weight of the stripe lying roughly on the diamond Fermi surface of a half-filled nearest neighbor tight-binding model. Here also, issues of interactions along a stripe were addressed and it was found that the distinct non-Fermi liquid properties of an interacting one-dimensional electron gas may be displayed also in directions not aligned with the stripes.

In the present paper we extend the work of Refs. 11 and 13 to look at a broader range of ordered structures. This is motivated by a search for a more comprehensive understanding of charge order in a doped antiferromagnet, but also by direct or indirect observations of structures which are not consistent with bond-aligned antiphase stripes. In the very lightly doped, nonsuperconducting phase of LSCO there are diffraction patterns consistent with diagonal stripes[14,15] instead of the bond-aligned stripes seen at higher doping. The transition between bond-aligned and diagonal stripes coincides with the superconductor to insulator transition at dop-

ing $x \approx 0.055$, suggesting a close link between the two properties. Within the noninteracting model considered here, we cannot directly address the connection between superconductivity and stripe orientation, but by comparing the predicted spectral weight of diagonal stripes with that observed in ARPES[16] we gain some insight into the nature of such diagonal stripes. Recently, there has also been indirect evidence from nuclear magnetic resonance (NMR),[17] thermal conductivity,[18] and magnetoresistance[19] measurements of an inhomogeneous charge structure in the electron-doped cuprates $(Pr,La)_{2-x}Ce_xCuO_4$ (PLCCO). However, in electron-doped materials there has been no evidence for incommensurate magnetism,[20] effectively ruling out the possibility of antiphase stripes. For this reason we have studied in-phase structures and compared the results to ARPES results on the $Nd_{2-x}Ce_xCuO_{4\pm\delta}$ (NCCO) family.[21]

Our results can be summarized as follows: As exemplified in Fig. 2 we find that the spectral weight of localized states is centered on the Brillouin zone (BZ) diagonals, given by $\cos(k_x)+\cos(k_y)=0$, independently of the magnitude of second and third nearest neighbor hopping t' and t'', as well as the shape and form of the charge "impurity." This shows why, in general, one may not expect any dramatic signature of stripes or other inhomogeneous electronic structure on the k-space distribution of low-energy spectral weight, as this is where the Fermi surface is located within a nearly half-filled tight-binding model which is dominated by nearest neighbor hopping. However, as shown in Figs. 7 and 12, and 16, a defining feature of the stripe states is that they have an energy which is within the Mott gap of the undoped system. Such in-gap states appear to be a common feature of the evolution of the band structures which doping as measured in ARPES and which we believe is a strong indication of an inhomogeneous charge distribution.[22]

We compare the dispersion and distribution of spectral weight of diagonal and bond-aligned stripes and find that pure diagonal stripes cannot reproduce the characteristic "Fermi arc" centered around the nodal region which is seen in ARPES on lightly doped LSCO. Instead we find that the spectral weight of a hole-doped diagonal stripe is concentrated to the "antinodal" BZ regions around $(\pi,0)$ with very little weight in the nodal region. In addition, the band width of states on a diagonal stripe is expected to be roughly $2|t'| \lesssim 0.2$ eV, which is inconsistent with the ARPES data where the band width of the in-gap states is of the order of 1 eV (assuming half is seen). However, it turns out that the spectral distribution and band width of bond-aligned stripes is qualitatively consistent with the ARPES data. For this reason we suggest that the diagonal stripe phase consists of stripes which are globally diagonal but locally bond aligned, a caricature of which are the "staircase stripes" shown in Fig. 4. Figure 6 shows the low-energy spectral weight, which is concentrated around the nodal region in a hole-doped array of staircase stripes.

An interesting aspect of these staircase stripes is the magnetic structure factors which depend on the ratio between the length of the bond-aligned segments, the "step" length l, and the distance between neighboring stripes d. As shown in Fig. 8, we find that the corresponding Bragg peaks can be classified in three main regimes. For $l \approx d$ there are two peaks corresponding to diagonal stripes along the $\hat{x}+\hat{y}$ direction at $(\pi \pm \delta_{\text{diag}}, \pi \mp \delta_{\text{diag}})$, for $l \approx 2d$ the diagonal peaks coexist with four peaks at $(\pi, \pi \pm \delta_{\text{col}})$ and $(\pi \pm \delta_{\text{col}}, \pi)$ corresponding to the response expected from bond-aligned stripes along the $\hat{x}$ and $\hat{y}$ directions, while for $l \gg d$ there are only the four bond-aligned peaks, but they are now shifted away slightly from the square lattice axes. The qualitative features are very similar to what is found from neutron scattering in LSCO as a function of doping,[15] although the relative incommensurability $\delta_{\text{diag}}/\delta_{\text{col}}$ is not quite accurately reproduced in the coexistence regime. Nevertheless, this suggests a scenario in which the stripes in the orthorhombic phase of LSCO are always locally bond-aligned, but in some sense globally diagonal with a crossover as the stripe spacing is decreased with increased doping and not a first-order transition as suggested by the neutron scattering data. Corroborating such a crossover scenario is the fact that the ARPES spectra evolve smoothly through the diagonal to bond-aligned stripe transition, and that the Fermi velocity in the nodal direction is roughly independent of doping, indicating that if the low-energy spectral weight is stripe related, the local character of the stripes does not change dramatically with doping.[16,23] In addition, the hole mobility at moderate temperatures changes by only a factor of 3 from very light ($x=0.01$) to optimal ($x=0.17$) doping, which is very naturally understood within a stripe model in which the local character of the stripes is roughly independent of doping.[24]

In Fig. 12 we show the band structure of a system with disordered in-phase stripes and in Fig. 11 the corresponding electron-doped low-energy spectral weight, which is in qualitative agreement with the ARPES data. The most interesting part of these results is the evolution of spectral weight in the nodal region, where at light doping (4%) there is in-gap spectral weight, which at higher doping (10%) broadens as a consequence of the shorter interstripe distance and reaches the Fermi surface. The evolution of the Fermi surface with doping can be reproduced in the mean-field theory of the Hubbard model with longer range hopping by allowing for a doping-dependent interaction U.[25] The difference within a stripe model is that the low-energy states are dynamically one dimensional, being localized transverse to the stripes (Fig. 13) and the existence of in-gap spectral weight. In addition we find that for in-phase stripes, in contrast to antiphase stripes, the chemical potential is likely to move into the upper Hubbard band with electron doping because the in-phase stripe states lie close to the upper and lower Hubbard bands (Fig. 14).

Finally, we present similar results from a calculation on a "bubble" phase where the doped charge is confined to small "zero-dimensional" droplets instead of the one-dimensional stripes. Bubbles would arise naturally instead of stripes in a $t-J$ model with long-range Coulomb repulsion in the limit $t \ll J$, because of the lower magnetic energy. Thus in the electron-doped materials, which appear to have "stronger" antiferromagnetism than the hole-doped materials, one may speculate that bubbles are favored over stripes. As far as the distribution of spectral weight is concerned (Figs. 15 and 16) there is little qualitative difference between bubbles and stripes. For the bubbles we find that the nodal spectral weight

broadens as the size of the bubbles increase with doping in analogy with the increasing density of stripes.

II. THE MODEL

We will consider a tight-binding model on a square lattice with first, second, and third nearest neighbor hopping together with a static potential that represents stripes or other charge structures. The Hamiltonian reads

$$H = -t\sum_{\langle rr'\rangle\sigma}(c^{\dagger}_{r,\sigma}c_{r'\sigma}+\text{H. c.}) - t'\sum_{\langle rr'\rangle'\sigma}(c^{\dagger}_{r,\sigma}c_{r'\sigma}+\text{H. c.}) - t''\sum_{\langle rr'\rangle''\sigma}(c^{\dagger}_{r,\sigma}c_{r'\sigma}+\text{H. c.}) + m\sum_{x,y,\sigma}\sigma(-1)^{x+y}V(x,y)c^{\dagger}_{x,y,\sigma}c_{x,y,\sigma}, \quad (1)$$

where $c_{r,\sigma}$ is the electron destruction operator at site $r=(x,y)$ and with spin $\sigma=\pm$. The hopping is given in a standard fashion, where $\langle rr'\rangle$ indicates nearest neighbors, $\langle rr'\rangle'$ next-nearest neighbors, and $\langle rr'\rangle''$ next-next nearest neighbors. In what follows we will use energy units such that $t=1$ and we take $t'/t<0$ and $t''/t>0$. The longer range hopping t' and t'' are included to qualitatively reproduce [Figs. 7(a) and 12(a)] the undoped ARPES measured band structure of the particular system studied. The physical intuition for the field m is that it is the energy cost of moving a hole from a stripe into the antiferromagnetic background and it is thus expected to be of the order of the spin exchange J. For simplicity, we will be using $m=t=1$ unless stated otherwise. We also use units such that the lattice constant is equal to one and $\hbar=1$.

The potential $m(-1)^{x+y}V(x,y)$ describes the collective field which defines the stripe order. We will use the simplest possible form and take $V(x,y)=1,0$ or -1, where $V(x,y)=1$ or -1 represent antiferromagnetic regions related by a π phase shift and $V(x,y)=0$ are the locations of the stripes. The case $V(x,y)=1$ for all x and y corresponds to the standard mean-field result of the Hubbard model at half-filling[26] giving an upper and lower Hubbard band separated by the Mott-Hubbard gap. Introducing regions where $V(x,y)=0$ will, in general, give rise to localized "impurity" states within the gap.

The object which was studied in detail in Ref. 13 is the site-centered antiphase stripe given by

$$V_{\text{stripe}}(x,y)=\begin{cases}1, & x>0\\ 0, & x=0\\ -1, & x<0,\end{cases} \quad (2)$$

and displayed graphically in Fig. 1(a). Here we also show two other charge structures, diagonal stripes and bubbles, which we will consider in more detail subsequently. In a real system we want to consider ordered or disordered arrays of structures such that at some finite doping the corresponding impurity states are partly occupied.

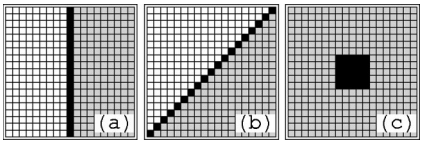

FIG. 1. Graphic representation of the potential $V(x,y)$ for various charge structures. Here, black corresponds to $V=0$, gray to $V=1$, white to $V=-1$ and each square represents a site (x,y) on the lattice. (a) is a bond-aligned antiphase stripe, (b) is an antiphase diagonal stripe, and (c) a bubble.

A. Spectral weight of localized states

Here we will show that a state $\psi^{\text{loc}}_{\vec{k}}$ localized on an impurity where the staggered field is zero has its spectral weight $|\psi^{\text{loc}}_{\vec{k}}|^2$ centered within a region m of the $\cos(k_x)+\cos(k_y)=0$ diamond, regardless of the values of the longer range hopping t' and t'' and the geometry of the impurity. This result is really a trivial consequence of the fact that the nearest neighbor hopping t connects the two sublattices of the staggered field while t' and t'' do not, or equivalently the symmetry or not of the dispersion, with respect to a shift of the momenta by scattering vector (π,π) of the staggered field.

We define a potential for an arbitrary impurity

$$V(x,y)=m(-1)^{x+y}, \quad \{x,y\}\notin \text{impurity}$$

$$V(x,y)=0, \quad \{x,y\}\in \text{impurity}, \quad (3)$$

and write the tight-binding dispersions

$$\varepsilon_{\vec{k}}=\varepsilon^{0}_{\vec{k}}+\varepsilon^{1}_{\vec{k}},$$

$$\varepsilon^{0}_{\vec{k}}=-2t[\cos(k_x)+\cos(k_y)],$$

$$\varepsilon^{1}_{\vec{k}}=-4t'\cos(k_x)\cos(k_y)-2t''[\cos(2k_x)+\cos(2k_y)]. \quad (4)$$

With this we solve for the eigenstates in the bulk

$$\psi_{\vec{k}}=a_{\vec{k}}e^{i\vec{k}\cdot\vec{x}}+b_{\vec{k}}e^{i(\vec{k}+\vec{\pi})\cdot\vec{x}}, \quad (5)$$

with energy

$$E_{\vec{k}}=\varepsilon^{1}_{\vec{k}}\pm\sqrt{(\varepsilon^{0}_{\vec{k}})^2+m^2}, \quad (6)$$

and ratio of coefficients

$$b_{\vec{k}}/a_{\vec{k}}=[-\varepsilon^{0}_{\vec{k}}\pm\sqrt{(\varepsilon^{0}_{\vec{k}})^2+m^2}]/m. \quad (7)$$

The localized state can be expanded in terms of the complete set of states $\psi_{\vec{k}}$, which are the solutions in the bulk. Clearly any state which is localized at the impurity must be sensitive to the staggered field. This means that it can only contain bulk solutions which are substantial superpositions of $\vec{k}$ and $\vec{k}+\vec{\pi}$, i.e., $b_{\vec{k}}/a_{\vec{k}}\sim 1$. From the expression, Eq. (7), for $b_{\vec{k}}/a_{\vec{k}}$ we find $\varepsilon^{0}_{\vec{k}}=1/2(a/b-b/a)m$ which implies that $\vec{k}$ is constrained to the volume $|\varepsilon^{0}_{\vec{k}}|\lesssim m$.

Figure 2 shows the full spectral weight of the three types of potentials displayed in Fig. 1, confirming our analytic re-

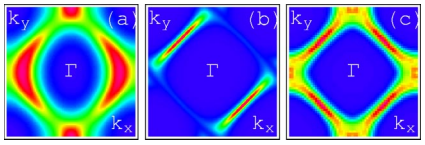

FIG. 2. (Color online) The spectral weight of various charge potentials as follows: (a) is a stripe along the y direction with $m=2, t'=-0.1, t''=0.1$, (b) is a diagonal stripe along $x+y$ direction with $m=0.5, t'=-0.1$, and $t''=0$, and (c) is a size 10×10 bubble with $m=1, t'=-0.1$, and $t''=0$.

sult. The broader distribution in k space for larger m is consistent with a shorter localization length in real space. Note also that for the diagonal stripe, in Fig. 2(b), the spectral weight is concentrated to those segments of the diamond which have momenta orthogonal to the stripe direction, a feature which will be important when analyzing diagonal stripes in the next section.

III. DIAGONAL STRIPES

One of the most interesting recent stripe-related observations is the diagonal stripes seen by quasielastic neutron scattering in the very underdoped insulating phase of LSCO.[14] As discussed in Sec. I, there is a crossover region where both diagonal and bond-aligned stripes appear to coexist, and which coincides with the rapid drop of the superconducting transition temperatures with decreasing doping,[15] pointing to a strong connection between stripes and superconductivity. On the other hand, we also noted that other properties, such as the nodal Fermi velocity and the hole mobility does not show any dramatic change across the bond aligned to diagonal transition.

What we can contribute to this discussion within our model is a comparison between the expected distribution of spectral weight between bond-aligned and diagonal stripes. It was already shown in Refs. 11 and 13 that a disordered bond-aligned stripe array can well reproduce the qualitative features of the near optimally doped samples. It is natural to do a similar analysis for the lightly doped samples $x=3-5\%$ studied by ARPES in Ref. 16. Experimentally it is found that the spectral weight in the antinodal, $(\pi,0)$, regions of the BZ, which is most prominent for the under- and optimally doped samples, is gapped away from the Fermi energy, and instead the low-energy spectral weight consists of disjoint arcs of "Fermi surface" centered near the nodal, $(\pi/2,\pi/2)$, regions. At first glance it is very tempting to identify these features with that shown in Fig. 2(b) for a diagonal stripe. However, although it is probably not completely ruled out that this simple picture is correct,[27] a closer study of the diagonal stripe reveals a serious problem. The problem is that for $t'<0$, a less then half-filled, i.e., hole-doped, diagonal stripe will have very little spectral weight in the nodal region, but only near the antinodal regions.

In order to understand this statement we can consider the dispersion of the diagonal and bond-aligned stripe as a function of the conserved momentum along the stripe. We will restrict ourselves to the limit $m\to\infty$ and numerically confirm

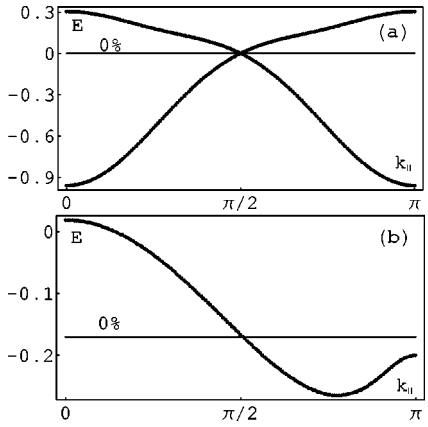

FIG. 3. Dispersions of in-gap states for $m=t=1$, $t'=-0.1$, and $t''=0$ for a bond-aligned stripe (a) along y with $k_\parallel=k_y$ and diagonal stripe (b) along $x+y$ with $k_\parallel=k_x+k_y$. Line marked "0%" indicates no-doped holes (half-filling).

the qualitative correctness for $m=1$. In this limit it is trivial to solve for the spectrum on the stripe because the problem reduces to a one-dimensional tight-binding chain. For the bond-aligned stripe there is the nearest neighbor hopping t while t'' acts as a next-nearest neighbor hopping, resulting in a dispersion

$$\varepsilon_{\mathrm{col}}(k_\parallel)\overset{m\to\infty}{=}-2t\cos(k_\parallel)-2t''\cos(2k_\parallel). \tag{8}$$

For the diagonal stripe the next-nearest neighbor hopping on the 2D lattice t' acts as a nearest neighbor hopping on the chain, giving a dispersion

$$\varepsilon_{\mathrm{diag}}(k_\parallel)\overset{m\to\infty}{=}-2t'\cos(k_\parallel). \tag{9}$$

Figure 3 shows numerically calculated dispersions for $m=1$, which agree qualitatively with the large m limit. Note that for the bond-aligned stripe, there is a folding of the BZ due to the antiferromagnetic scattering along the stripe direction, which is absent for the diagonal stripe. The conclusion we want to draw from these dispersions is that for the diagonal stripe at any finite hole doping, the momenta of filled states which may contribute to the low-energy spectral weight are confined to $k_\parallel>\pi/2$. From the distribution of spectral weight for a diagonal stripe, in Fig. 2(b), we find that this implies that there is very little spectral weight in the nodal regions. We can easily convince ourselves that this distribution of the spectral weight of a diagonal stripe is a general consequence of the fact that a state with some momentum $k_\parallel$ will, as shown in Sec. II A, have its spectral weight concentrated in the intersection of the line $k_x+k_y=k_\parallel$ with the $\cos(k_x)+\cos(k_y)=0$ diamond. This implies that for $|k_\parallel|=\pi$ the weight will spread out over the whole intersection, which is a line, while for $|k_\parallel|<\pi$ the weight will be concentrated to the two points of intersection.

These results for the distribution of the spectral weight of a hole-doped diagonal stripe may be contrasted with that of a bond-aligned stripe. Here we find from Fig. 3(a) complemented with Fig. 2(a) that for finite hole doping, the spectral weight may be spread out over the whole diamond. The de-

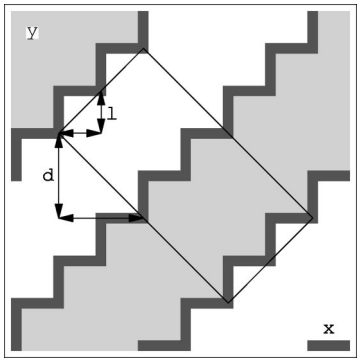

FIG. 4. Graphical representation of a staircase stripe defined by the step length l and the stripe distance d. The rectangle indicates a primitive cell. The potential $V(x,y)$ is given by $V=0$ for darker gray, $V=1$ for light gray, and $V=-1$ for white.

tails, of course, depend on the doping, the parameters used, and on the density of stripes. The latter being particularly important in that for a short interstripe distance the stripe states will overlap and form bands of momenta transverse to stripes (see Fig. 14).

One might, in an effective model such as this, attempt to fit the experimental data by taking $t'>0$ which would allow for spectral weight concentrated in the nodal region. However the ARPES data for the lightly doped samples indicate that most of the additional weight introduced with doping is, in fact, in the antinodal region only that it is gapped away from the Fermi surface. If we take $t'>0$ we would vacate the antinodal states and we would not be able to reproduce this qualitative feature. Related to this there is a more quantitative problem for a diagonal stripe as contrasted with the ARPES data, which should be more general than our model, namely that the bandwidth of a purely diagonal stripe is expected to be proportional to t'. Values of t' in the literature are less than 0.1 eV, implying a bandwidth $W_{\text{diagonal}}<0.2$ eV, whereas the bandwidth from the in-gap states seen in ARPES can be estimated at $W_{\text{in-gap}}\lesssim 1$ eV, which looks more consistent with the band width $W_{\text{col}}\sim 2t$ of bond-aligned stripes. To summarize, we find that *pure diagonal stripes are not consistent with the ARPES data of lightly doped LSCO*.

A. Staircase stripes

Given the difficulties with matching the model using a diagonal stripe configuration to the ARPES data it is instead tempting to look at bond-aligned stripes. Now, we know from neutron scattering that bond-aligned stripes are not seen in these very lightly doped materials, but only diagonal stripes. This led us to investigating the properties of stripes which are locally bond-aligned but globally diagonal. A natural and most simple candidate for such a construction is a "staircase" stripe. We can define a staircase stripe along the $x+y$ direction, but letting it run alternately along the $\hat{x}$ and $\hat{y}$ directions with some step length l. For an ordered array of such staircase stripes we also introduce a stripe distance d defined according to Fig. 4. In the case of antiphase stripes, the potential has the symmetries

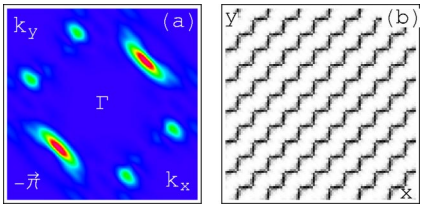

FIG. 5. (Color online) An ordered array of staircase stripes with $l=8$ and $d=8$, using $t=m=1$, $t'=-0.1$, and $t''=0$. Momentum space (a) and real space (b) spectral weight integrated over an energy window of 0.2 around the Fermi energy at 4% hole doping. The full system size is 256×256 while in (b) is shown a 100×100 section.

$$V(x+l,y+l)=V(x,y),$$

$$V(x+d,y-d)=-V(x,y), \tag{10}$$

which also give the primitive cell as indicated in the figure. The same symmetries hold true for the full potential of Eq. (1) which is simply multiplied by a factor $(-1)^{x+y}$ to account for the staggered field.

We will return to magnetic structure factors of such staircase stripes below, but it is easy to see that as long as $l\leqslant d$ the main magnetic diffraction peaks of such a staircase stripe are equivalent to an array of purely diagonal stripes with the interstripe distance $2d$ along the x and y direction.

We turn now to the distribution of spectral weight of staircase stripes. As an example we look at a system with $l=8$ and $d=8$, where d is chosen such that the magnetic structure factor has main peaks at $(\pi\pm\delta/\sqrt{2},\pi\mp\delta/\sqrt{2})$ with $\delta/\sqrt{2}=1/32$, which corresponds roughly to the $\delta\approx1/25$ seen in neutron scattering at 4% doping. We diagonalize this system numerically to find the single particle eigenstates $\psi_\alpha(\vec{k})$, with energies E_α, in terms of which we calculate the single particle spectral function

$$A(\vec{k},\omega)=\sum_\alpha |\psi_\alpha(\vec{k})|^2\delta(E_\alpha-\omega), \tag{11}$$

where $\delta(E_\alpha-\omega)$ is the Kronecker delta, and the local density of states

$$R(\vec{r},\omega)=\sum_\alpha |\psi_\alpha(\vec{r})|^2\delta(E_\alpha-\omega), \tag{12}$$

with $\psi_\alpha(\vec{r})=1/L_xL_y\Sigma_{\vec{k}}e^{i\vec{k}\cdot\vec{r}}\psi_\alpha(\vec{k})$ being the eigenfunctions in real space. Figure 5 shows spectral weight distribution in k space and real space when integrated over an energy window $\Delta\omega=0.2$ around the Fermi energy at 4% doping, i.e., calculating

$$I(\vec{k})=\int_{E_F-\Delta\omega/2}^{E_F+\Delta\omega/2}A(\vec{k},\omega)d\omega, \tag{13}$$

and

$$R(\vec{r})=\int_{E_F-\Delta\omega/2}^{E_F+\Delta\omega/2}R(\vec{r},\omega)d\omega. \tag{14}$$

We find that the low-energy spectral weight is concentrated near the nodal region. It is highly anisotropic with most of

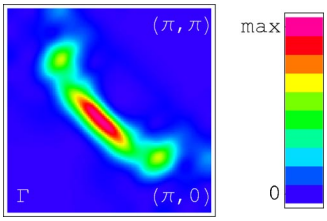

FIG. 6. (Color online) Same as Fig. 5 but symmetrized with respect to the stripe orientation and in the first quadrant of the BZ. Shown is also the intensity map which has a linear scale.

the spectral weight parallel to the overall stripe direction along $x+y$ in contrast to the pure diagonal stripe shown in Fig. 2(b). We have tried making the step length l shorter, which gives results closer to the pure diagonal stripe with most of the spectral weight in the antinodal region. In Fig. 6 the results are symmetrized with respect to the stripe direction, so that $(\pi,\pi)=(\pi,-\pi)$, etc. Here, the disjoint features merge into a single piece of "Fermi arc" in each quadrant of the BZ, similar to what is seen in ARPES. Note that in Fig. 5(b) it is not the stripe potential $V(x,y)$ which is plotted, but the amplitude in real space of the low-energy states. Not surprisingly, these follow the potential quite closely, but there is some leakage of spectral weight into the antiferromagnetic regions which appears to smooth the kinks and make the stripes more diagonal. An indication that the staircase stripes are just a caricature with the real stripes probably being smoother, but nevertheless are locally closer to bond aligned than to diagonal.

We can gain a better understanding of these results for the low-energy spectral weight by studying the spectral function, $A(\vec{k},\omega)$, over a broader energy window along the high-symmetry directions, as shown in Fig. 7. The qualitative features of the spectral weight deriving from the staircase stripes can be directly linked to the properties of ordinary

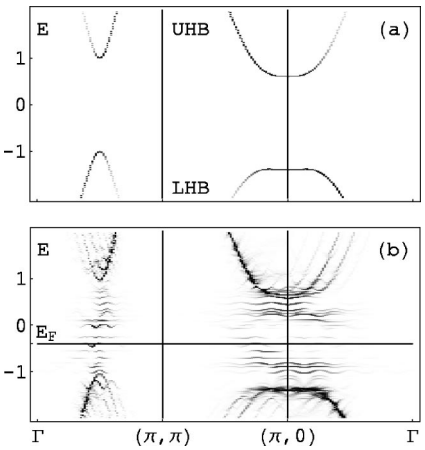

FIG. 7. Band structure of system with $t=m=1$, $t'=-0.1$, and $t''=0$ for (a) no stripes and (b) with staircase stripes as in Fig. 5. UHB and LHB indicate upper and lower Hubbard bands, respectively, and E_F is the Fermi energy at 4% hole doping. The spectral weight is indicated by the intensity, but on a nonlinear scale that exaggerates low-intensity features. (b) is symmetrized with respect to the stripe direction.

bond-aligned stripes. The high energy (away from E_F) spectral weight is concentrated around the antinodal, $(\pi,0)$, region whereas the low-energy spectral weight close to the Fermi energy is focused to the nodal region around $(\pi/2,\pi/2)$. This is what we would find from a lightly hole doped bond-aligned stripe with the dispersion in Fig. 3(a), given the fact that the spectral weight is concentrated to the intersection of $k_\parallel=k_x$ or k_y with the BZ diamond.

1. Magnetic structure factors of staircase stripes

In the previous section we found a qualitative agreement of the spectral distribution of staircase stripes with that seen experimentally in lightly doped LSCO. Here, we had to restrict ourselves to staircase stripes with step length l less than the stripe distance d as defined in Fig. 4 in order to have a magnetic structure factor which corresponds to diagonal stripes. A natural extension is to study also stairs with $l>d$. Certainly, in limit $l\gg d$ we expect very little influence from the kinks and the system will become equivalent to that of bond-aligned stripes, both for the spectral distribution and structure factors. We found that the distribution of spectral weight could be rationalized in terms of bond-aligned stripes already for the system with $l=d$ so that for $l>d$ we would not expect any qualitative difference between the spectral distribution of staircase stripes with that of bond-aligned stripes studied in the earlier work.[11,13] What is more interesting is to study the magnetic structure factor, which is sensitive to the global properties of the system.

Physically, the relevant entity is the magnetic structure factor which is the amplitude $|S^z(\vec{q})|^2$ of the Fourier transformed spin density, which at zero temperature reads

$$S^z(\vec{q}) = 1/L^2 \sum_{\vec{r},\alpha,\sigma} e^{i\vec{q}\cdot\vec{r}}\sigma|\psi_{\alpha\sigma}(\vec{r})|^2\Theta(E_F-E_\alpha). \qquad (15)$$

However, for a large system, such as for disordered stripes, this is difficult to calculate because of the need to diagonalize the system. Much simpler to find is the amplitude squared of the Fourier transform of the stripy potential $(-1)^{x+y}V(x,y)$. We have checked for several ordered stripe arrays that close to half-filling the two calculations give very similar results. This is expected because the difference is roughly the amplitude on the stripes, which is zero for the potential, but slightly different from zero for the actual spin density because of the occupied stripe states.

Using the symmetry properties of a staircase stripe, Eq. (10), we find that $V(k_x,k_y)$ can only have nonzero components for

$$k_x + k_y = \frac{2\pi}{l}N, \quad N \in \text{integer} \qquad (16)$$

$$k_x - k_y = \frac{2\pi}{2d}N', \quad N' \in \text{odd integer}. \qquad (17)$$

Figure 8 shows the structure factors of three different stripe realizations, $l=d$, $l=2d$, and $l=5d$. We find three very distinct diffraction patterns, where the first corresponds to diagonal stripes, the second looks like diagonal stripes coexisting

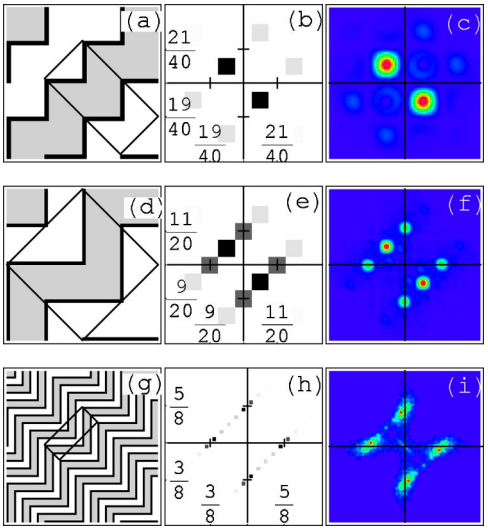

FIG. 8. (Color online) The magnetic structure factors of the three different regimes of staircase stripes discussed in text. The left column shows the unit cells which in (a) is 80×80 with step length $l=20$ and stripe distance $d=20$, in (d) is 40×40 with $l=20$, $d=10$ and in (g) is 80×80 with $l=20$, $d=4$. The stripes where the potential is zero are black, the two π-shifted domains of the antiferromagnetic order and the rectangles are primitive cells are gray and white. The middle column, (b), (e), and (h), shows the corresponding structure factors in reciprocal lattice units centered around $(1/2,1/2)=(\pi,\pi)$. The right column, (c), (f) and (i), give the structure factors of a sum over ten 80×80 disordered configurations of the corresponding ordered states to the left, where the length of the legs and the distance between stripes are allowed to vary with a flat random distribution without allowing stripes to come closer than one site separation. The width of the peaks of the right column is simply related to the fraction of the BZ viewed, given that in all calculations, the same correlation length is used.

with both vertical and horizontal bond-aligned stripes, and the last looks like vertical and horizontal stripes, but with an orientation which deviates slightly from bond-aligned. We also show diffraction patterns of samplings over disordered stripe configurations where we find that, in general, only the primary peaks survive with secondary, lower intensity peaks, getting washed out, although this does not happen for the second configuration with coexisting bond-aligned and diagonal peaks. We have also studied stripe arrays with larger unit cells where l is not an integer factor of d. For disordered realizations it appears that these roughly fall into one of the three characteristic regimes, with only a quite narrow window of $l\approx2d$ showing both diagonal and bond-aligned peaks of appreciable amplitude.

These results for the diffraction pattern of staircase stripes appear qualitatively very similar to what is seen in neutron diffraction experiments on LSCO in the low-temperature orthorhombic (LTO) phase.[15] In the nonsuperconducting phase at very low doping ($x\lesssim6\%$), peaks are consistent with diagonal stripes, whereas at higher doping ($x\approx10-13\%$) a pattern is consistent with stripes that are close to bond aligned but shifted by a few degrees from the tetragonal axes. More recently it was found that very close to the insulator to superconducting transition ($x\approx6\%$) both patterns coexist. This may suggest that the stripes in the LTO phase of LSCO are always of the staircase type and that the transition between bond-aligned and diagonal stripes is a crossover from a regime where $l>2d$ to one where $l<2d$. Particularly interesting are the more detailed experimental data from neutron scattering on the underdoped superconducting regime $x\approx10\%$. From the staircase stripe scenario we would expect a larger angle of deviation from the tetragonal axes than for the samples with higher doping, possibly together with secondary peaks in the diagonal direction or on the tetragonal axes as shown in Fig. 9.

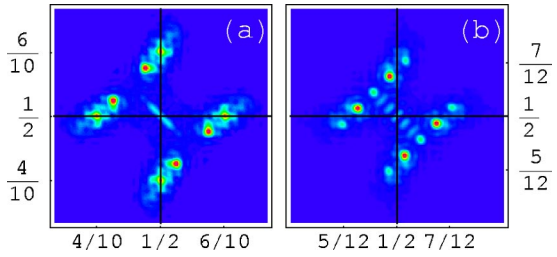

FIG. 9. (Color online) Magnetic structure factors of disordered realizations of staircase stripes with $l=20$ and (a) $d=5$ and (b) $d=6$, which could roughly correspond to 10% and 8% doping, respectively.

We should note that the correspondence between the experiment and our results for staircase stripes is not perfect. In particular there appears to be a discrepancy with the relation between the "incommensurabilty" δ, defined as the shift of a peak from (π,π), of the diagonal and bond-aligned components. For the staircase stripes we find $\delta_{\mathrm{diag}}=\delta_{\mathrm{col}}/\sqrt{2}$, whereas experimentally is seen $\delta_{\mathrm{diag}}\approx\delta_{\mathrm{col}}$. The former relation follows directly from the symmetry of the stripy potential, Eq. (17), and consequently is not sensitive to small changes of the potential such as for instance smoothing of the kinks.

IV. IN-PHASE STRIPES

We now turn to a study of the spectral weight distribution of in-phase stripes. As discussed in Sec. I there is indirect evidence for an inhomogeneous charge distribution in the electron-doped PLCCO.[17–19] In fact, the possibility of in-phase stripes had already been suggested from the theory for hole-doped stripes at lower hole densities.[28]

The experimental hallmark of antiphase stripes is the incommensurate magnetism detected by neutron diffraction, where the weight is shifted away from the antiferromagnetic ordering vector $\vec{Q}=(\pi,\pi)$. A system with ordered in-phase stripes, on the other hand, will have a main diffraction peak at the antiferromagnetic (AF) ordering vector with satellites at positions shifted by integer multiples of $2\pi/d$, where d is the distance between stripes. However, if the stripes are not static and ordered, but fluctuating or disordered, the satellite peaks will easily be washed out and the weight absorbed into the AF peak. Figure 10 shows the amplitude squared of the Fourier transform of the stripe potential $(-1)^{x+y}V(x,y)$ along the transverse direction for ordered and disordered antiphase and in-phase stripes and for the charge density represented

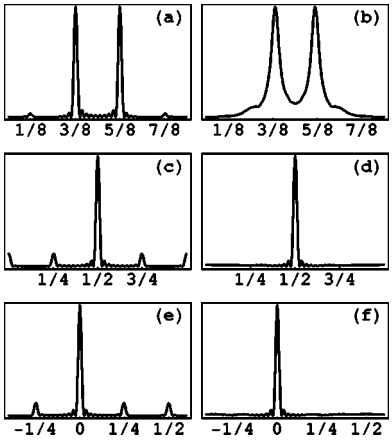

FIG. 10. Structure factors (in arbitrary units) of spin and charge density for antiphase and in-phase stripes as a function of momentum transverse to the stripes in r.l.u. The left column shows ordered arrays with stripe distance $d=4$ and the right disordered with a flat distribution $d=2-6$. (a) and (b) show the spin order for antiphase stripes, (c) and (d) show the spin order for in-phase stripes, and (e) and (f) show the charge order which is independent of the type of stripe. In all figures a finite correlation length of 40 sites is used and the disordered systems are averaged over 1000 samples.

by $|V(x,y)|$. For the charge order there is no difference between antiphase and in-phase stripes. Nevertheless, charge order is more difficult to detect, even for systems with static order. The reason for this is that neutrons do not couple directly to the charge order and that the superlattice peaks related to charge stripe order arise from modulations of the uniform charge density, $\vec{Q}=(0,0)$, which dominates the structure factor. As shown in Fig. 10, these peaks are also readily destroyed by disorder. (In fact, the charge structure factor as estimated here is equivalent to the spin structure factor of in-phase stripes but shifted by π.) Direct signatures of in-phase stripes from neutron or x-ray scattering will thus be much more difficult to find, most likely requiring a stripe ordered material.

Nevertheless, given the indirect indications for the existence of in-phase stripes in electron-doped cuprates, it may be interesting to study the implications of such structures to the distribution of spectral weight. In Fig. 11 is shown the integrated spectral weight close to the Fermi energy for disordered in-phase stripes with interstripe distances 9–15 with

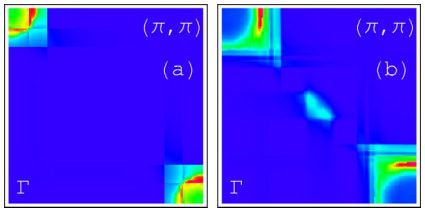

FIG. 11. (Color online) Spectral weight close to E_F (window 0.2) of disordered in-phase stripes with $t=m=1$, $t'=-0.2$, and $t''=0.1$. Mean stripe distance in (a) is 12 with E_F at 4% doping and in (b) mean distance is 4 with E_F at 10% doping. The results are symmetrized with respect to the stripe direction. The system size is 320×320.

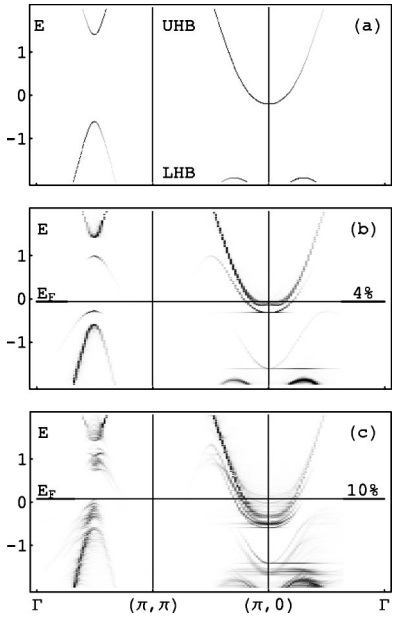

FIG. 12. The band structure of the system with $t=m=1$, $t'=-0.2$, and $t''=0.1$ and in-phase stripes as in Fig. 11. (a) is no stripes, (b) mean stripe period 12 and (c) mean stripe period 4.

mean 12 and 1–7 with mean 4 for a system with $t=m=1$, $t'=-0.2$, and $t''=0.1$. The parameters t' and t'' are chosen such as to roughly reproduce the band structure of the undoped system seen in ARPES on the electron-doped NCCO[21] with the smallest spectral gap at $(\pi/2,\pi/2)$ as shown in Fig. 12(a). The density of stripes is assumed to be roughly as in the hole-doped materials with stripe spacing d given by the doping n according to $n\approx1/2d$, which for electron doping corresponds to 3/4-filled stripes.

Clearly these results reproduce the experimental Fermi surface quite well; at light doping there are patches of spectral weight around $(\pi,0)$ while at higher doping the weight starts to look more like a full Fermi surface closed around (π,π), but with weight missing at "hot-spots," where the putative Fermi surface cuts the BZ diagonal (diamond). Similar results have been reproduced by the mean-field theory of the $t-t'-t''-U$ Hubbard model by allowing for a doping-dependent U.[25] This is, in fact, the model we consider, but without the stripes and with a magnitude of the staggered field m which depends on U. Here, we keep the parameters fixed, but vary the stripe spacing as a function of doping. There are, however, very distinct differences between the implications of the two scenarios. In the stripe model there are midgap states, not present for the model with a uniform staggered field. This is particularly visible for the lightly doped system, Fig. 12(b), where along the $\Gamma=(0,0)$ to (π,π) direction there is spectral weight between E_F and the lower Hubbard band. Precisely, such a feature is seen in the ARPES data for the 4% doped sample. Secondly, the low-energy states of the stripe model are dynamically one dimensional, i.e., they are localized transverse to a stripe but have a well-defined momentum along the stripe, as shown in Fig. 13. Thus, one of the main conclusions is that the distribution of low-energy spectral weight, the "Fermi surface," may be

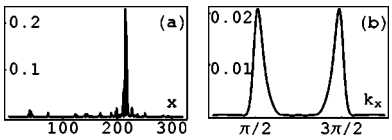

FIG. 13. Example of a single state ψ of system in Fig. 12(c), with energy $E \approx 0$ and momentum along stripe direction $k_y = \pi/2$, showing localization in the transverse stripe direction. In (a) the real space amplitude $|\psi(x,y)|^2$ is shown as a function of transverse direction x for arbitrary y and in (b) the k-space amplitude $|\psi(k_x)|^2$. We can estimate a localization length $\xi \approx 2$ from the real space peak amplitude.

indistinguishable from a homogeneous two-dimensional system even though the states are dynamically one dimensional.

Let us now look at how we can understand this evolution of spectral weight with doping and corresponding increasing stripe density from the properties of a single in-phase stripe. Figure 14 shows the spectra of systems with sparse, mean distance 12, and dense, mean distance 4, stripes. For the sparse stripes, Fig. 14(a), the stripe states are clearly visible as the isolated in-gap bands. Because there is no broadening of the stripe states, the stripes are clearly sufficiently far apart as to be effectively independent. We find that in-phase stripes at moderate m have a band structure that is distinctly different from that of antiphase stripes, as shown in Fig. 3(a), with the former staying close to the upper and lower Hubbard bands.[29] (We have checked that in the limit $m \to \infty$, where in-phase and antiphase stripes are equivalent, the dispersion Eq. (8) is correctly reproduced also for in-phase stripes.) As the stripe density is increased, the stripe states will overlap and form bands transverse to the stripes, in Fig. 14(b), with states from the lower branch crossing the Fermi energy. Because of disorder, these states may nevertheless be strongly localized as shown in Fig. 13.

An important point about in-phase stripes, which is demonstrated here is that the chemical potential may move as a function of doping and is not necessarily pinned within the gap. This is particularly evident in comparing the 0% and 4% samples, as shown in Figs. 12(a) and 12(b), where in the former the chemical potential is in the gap ($-0.6 < \mu < -0.2$), whereas in the latter it has moved up to cut the upper Hubbard band ($\mu \approx 0$). The motion of the chemical potential is a necessary consequence of the dispersion of in-phase stripes as shown in Fig. 14(a), with the stripe states "hugging" the upper and lower Hubbard bands. This is in sharp contrast to antiphase stripes (Figs. 7 and 3), where the spectral weight of the stripe states is "midgap," implying that the chemical potential may stay fixed with doping. Motion of the chemical potential with doping is thus not necessarily an indication of the absence of stripes.[21,30]

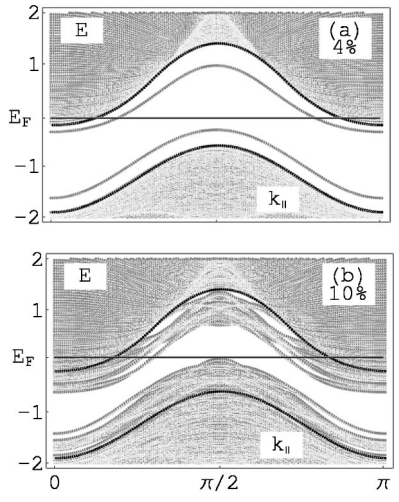

FIG. 14. Spectrum for $|E| < 2$ of in-phase stripe systems as in Fig. 12 with mean stripe period 12 in (a) and 4 in (b) as a function of momentum $k_\parallel = k_y$ parallel to the stripe direction y. The black curves indicate the bounds of the upper and lower Hubbard bands for the corresponding system without stripes.

A. Bubbles

Because of the lack of direct diffraction evidence for stripes, one may be free to speculate on other forms of charge order in these materials. The microscopic motivation for stripe formation is the tendency of the antiferromagnet to expel extra charge which will disrupt the local antiferromagnetism. The formation of stripes is then a compromise between the minimizing of the magnetic energy by concentrating the holes, of the kinetic energy by allowing holes to delocalize along the stripes, and possibly of the charging energy due to long-range Coulomb repulsion by not allowing a macroscopic charge inhomogeneity.[31]

However, if the magnetism is relatively stronger than the kinetic energy contribution, the system may prefer to keep the extra charge in zero-dimensional "bubbles" [see Fig. 1(c)] in order to minimize the disruption of the local magnetic order.[32] Roughly speaking, for a completely filled stripe with two electrons per site on a one-site wide stripe there are three bad bonds where the spin exchange is destroyed per stripe site, while for a bubble there are only two bad bonds per site. (The sites on the perimeter of the bubble have three bad bonds.) In addition, because of charging energy, the bubbles would have to be limited to a microscopic size. Clearly, the putative stripes or bubbles are not completely filled in the electron-doped materials, due presumably to kinetic energy considerations, as this would imply an insulating system.

For simplicity we look at square bubbles, and because this problem is fully two dimensional, with a large unit cell, we only consider ordered systems. For the previous study of in-phase stripes we chose stripe spacings and fillings that were based on the corresponding values for antiphase stripes in the hole-doped systems. For the bubble phase we have even less to guide us on how to choose the size and period of the bubbles. However, assuming that the putative bubble formation is due to competition between the magnetic energy and the charging energy, we can get a simple estimate of the variation of bubble size with doping, completely ignoring the kinetic energy. It is easy to see that for a classical antiferromagnet, we decrease the number of bad bonds that are not connecting antiferromagnetically aligned spins by two per doped electron by forming bubbles instead of a homogeneous (Wigner crystal) distribution of the doped charge. This

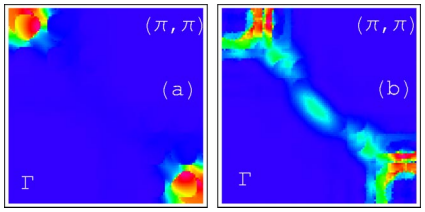

FIG. 15. (Color online) Spectral weight within energy window 0.2 of E_F of ordered array of bubbles with $t=m=1$, $t'=-0.2$, and $t''=0.1$. In (a) the unit cell is 12×12 with the bubble size 4×4 and E_F is at 4% electron doping. In (b) the unit cell is 20×20 with the bubble size 10×10 and E_F at 10% doping.

gives an energy gain $E_{\mathrm{AF}}\sim -JL^2$, where J is the AF exchange, which is typically of the order of 0.1 eV, and L is the linear dimension of the bubble. The charging energy due to moving L^2 electrons together from a closest distance $1/n$ to a closest distance 1 is given by $E_{\mathrm{Q}}\sim QL^3(1-n)$, assuming a Coulomb interaction $V=Q/r$ with r in units of the lattice constants. Here $Q=(e^2/4\pi\epsilon_0\epsilon a)\approx 0.3$ eV, assuming a lattice constant of $a=5$ Å and a dielectric constant $\epsilon=10$.[33] Minimizing the total energy with respect to the bubble size L gives $L\sim[J/Q(1-n)]$, so that for small doping, n, we find the bubble size proportional to the doping. The prefactor J/Q seems somewhat on the small side, but does not rule out bubbles as a viable scenario. Clearly large J, or "strong" antiferromagnetism, will favor the bubble scenario. This is the reason why we suggest it for the electron-doped materials, which in general show antiferromagnetism over a much wider doping range than do hole-doped materials.

For the calculations presented here we choose a bubble size $L=100n$ and let the distance between bubbles vary with doping, such as to correspond to roughly 3/4-filled bubbles. Figure 15 shows the integrated spectral weight near the Fermi energy for two realizations, at 4% and 10% doping, and in Fig. 16, the corresponding band structure. The results are qualitatively similar to what was found for in-phase stripes. The evolution of the weight near $(\pi,0)$ does not depend crucially on the bubbles but can be understood from increasing the filling of the upper Hubbard band. The nodal weight near $(\pi/2,\pi/2)$ on the other is clearly an effect of the additional states deriving from the bubbles.

V. CONCLUSIONS

We have investigated the distribution of electronic spectral weight in various charge ordered antiferromagnets. We find that the spectral weight of states localized on a stripe or other charge structure is centered on and spread out over the Brillouin zone diagonals $[\cos(k_x)+\cos(k_y)=0]$. The distribution of spectral weight close to the Fermi energy may thus look fully two dimensional and practically indistinguishable from a homogeneous system even though the low-energy states are dynamically one or even zero dimensional, localized on stripes or bubbles. On the other hand, the stripe states will, in general, lie within the energy gap of the undoped system making the appearance of "in-gap" states an expected consequence of an inhomogeneous charge distribution.

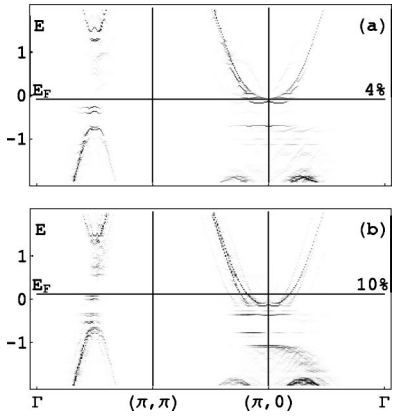

FIG. 16. The band structure of the system in Fig. 15. The band structure without bubbles is the same as in Fig. 12(a).

We find that pure diagonal stripes cannot reproduce the distribution of spectral weight found in ARPES on the very underdoped LSCO in the "diagonal stripe" phase. Instead we introduce "staircase" stripes, which are locally vertical or horizontal, but globally diagonal, in terms of which the qualitative features of the ARPES data are readily reproduced. Calculating the structure factors of such staircase stripes, we find that these evolve with doping and corresponding stripe density in a way that is very similar to the neutron scattering data in the LTO phase of LSCO over the whole doping range from very light to optimal. The results suggest that the horizontal to diagonal stripe transition may be a crossover between a regime where the typical length of straight (horizontal or vertical) stripe segments is longer than the interstripe spacing to one where it is shorter and that the stripes are always locally bond-aligned in LSCO.

We find that in-phase stripes can qualitatively reproduce the ARPES data and evolution with doping in the electron-doped cuprate NCCO. Particularly revealing is the spectral weight in the nodal region, near $(\pi/2,\pi/2)$, where at low doping there is "stripy" spectral weight in the gap, which at higher doping broadens as a result of increased stripe density and crosses the Fermi energy. For in-phase stripes, in contrast to antiphase stripes, we find that the in-gap states lie close to the upper and lower Hubbard bands implying that the chemical potential is likely to move with doping. We also consider bubble structures and find that these produce similar results for the distribution of spectral weight to that of in-phase stripes by allowing the bubble size to grow with doping. We argue that these may be an alternative to stripes in the electron-doped materials where there is a broad doping range with antiferromagnetic order.

ACKNOWLEDGMENTS

The author would like to thank S.A. Kivelson and Y. Ando for valuable discussions. This work was supported by the Swedish Research Council.

*Electronic address: mgranath@fy.chalmers.se

[1] For a review, see E. W. Carlson, V. J. Emery, S. A. Kivelson, and D. Orgad, in *Concepts in High Temperature Superconductivity*, edited by K. H. Bennemann and J. B. Ketterson, The Physics of Conventional and Unconventional Superconductors (Springer-Verlag, New York, 2003)

[2] V. J. Emery, S. A. Kivelson, and O. Zachar, Phys. Rev. B **56**, 6120 (1997).

[3] V. J. Emery, E. Fradkin, S. A. Kivelson, and T. C. Lubensky, Phys. Rev. Lett. **85**, 2160 (2000).

[4] E. Arrigoni, E. Fradkin, and S. A. Kivelson, cond-mat/0309572.

[5] For a review focused on experimental evidence of stripes, see S. A. Kivelson, E. Fradkin, V. Oganesyan, I. P. Bindloss, J. M. Tranquada, A. Kapitulnik, and C. Howald, Rev. Mod. Phys. **75**, 1201 (2003).

[6] S. A. Kivelson, E. Fradkin, and V. J. Emery, Nature (London) **393**, 550 (1998).

[7] N. Ichikawa, S. Uchida, J. M. Tranquada, T. Niemöller, P. M. Gehring, S.-H. Lee, and J. R. Schneider, Phys. Rev. Lett. **85**, 1738 (2000).

[8] Indications of a 1D Fermi surface in LSCO [X. J. Zhou, P. Bogdanov, S. A. Kellar, T. Noda, H. Eisaki, S. Uchida, Z. Hussain, and Z.-X. Shen, Science **286**, 268 (1999)] were later revised to appear more 2D [X. J. Zhou, T. Yoshida, S. A. Kellar, P. V. Bogdanov, E. D. Lu, A. Lanzara, M. Nakamura, T. Noda, T. Kakeshita, H. Eisaki, S. Uchida, A. Fujimori, Z. Hussain, and Z.-X. Shen, Phys. Rev. Lett. **86**, 5578 (2001)].

[9] See, for example, P. W. Anderson, *The Theory of Superconductivity in the Cuprates* (Princeton University Press, Princeton, NJ, 1997); R. B. Laughlin, Phys. Rev. Lett. **79**, 1726 (1997); D. Orgad, S. A. Kivelson, E. W. Carlson, V. J. Emery, X. J. Zhou, and Z. X. Shen, *ibid.* **86**, 4362 (2001).

[10] For a review on ARPES, see A. Damascelli, Z. Hussain, and Z.-X. Shen, Rev. Mod. Phys. **75**, 473 (2003).

[11] M. Salkola, V. J. Emery, and S. A. Kivelson, Phys. Rev. Lett. **77**, 155 (1996).

[12] We will use the term "bond-aligned stripes" to indicate stripes which are aligned with the Cu-O bond direction or the bonds of the square lattice in the model Hamiltonian. Such stripes are commonly refered to as vertical or horizontal but here we may or may not want to distinguish between the two.

[13] M. Granath, V. Oganesyan, D. Orgad, and S. A. Kivelson, Phys. Rev. B **65**, 184501 (2002).

[14] S. Wakimoto, G. Shirane, Y. Endoh, K. Hirota, S. Ueki, K. Yamada, R. J. Birgeneau, M. A. Kastner, Y. S. Lee, P. M. Gehring, and S. H. Lee, Phys. Rev. B **60**, R769 (1999).

[15] M. Fujita, K. Yamada, H. Hiraka, P. M. Gehring, S. H. Lee, S. Wakimoto, and G. Shirane, Phys. Rev. B **65**, 064505 (2002).

[16] T. Yoshida, X. J. Zhou, T. Sasagawa, W. L. Yang, P. V. Bogdanov, A. Lanzara, Z. Hussain, T. Mizokawa, A. Fujimori, H. Eisaki, Z.-X. Shen, T. Kakeshita, and S. Uchida, Phys. Rev. Lett. **91**, 027001 (2003).

[17] F. Zamborszky, G. Wu, J. Shinagawa, W. Yu, H. Balci, R. L. Greene, W. G. Clark, and S. E. Brown, Phys. Rev. Lett. **92**, 047003 (2004).

[18] X. F. Sun, Y. Kurita, T. Suzuki, S. Komiya, and Y. Ando, Phys. Rev. Lett. **92**, 047001 (2004).

[19] P. Fournier, M.-E. Gosselin, S. Savard, J. Renaud, I. Hetel, P. Richard, and G. Riou, cond-mat/0309144.

[20] K. Yamada, K. Kurahashi, T. Uefuji, M. Fujita, S. Park, S.-H. Lee, and Y. Endoh, Phys. Rev. Lett. **90**, 137004 (2003).

[21] N. P. Armitage, F. Ronning, D. H. Lu, C. Kim, A. Damascelli, K. M. Shen, D. L. Feng, H. Eisaki, Z.-X. Shen, P. K. Mang, N. Kaneko, M. Greven, Y. Onose, Y. Taguchi, and Y. Tokura, Phys. Rev. Lett. **88**, 257001 (2002).

[22] S. A. Kivelson and V. J. Emery, Synth. Met. **80**, 151 (1996).

[23] X. J. Zhou, T. Yoshida, A. Lanzara, P. V. Bogdanov, S. A. Kellar, K. M. Shen, W. L. Yang, F. Ronning, T. Sasagawa, T. Kakeshita, T. Noda, H. Eisaki, S. Uchida, C. T. Lin, F. Zhou, J. W. Xiong, W. X. Ti, Z. X. Zhao, A. Fujimori, Z. Hussain, and Z.-X. Shen, Nature (London) **423**, 398 (2003).

[24] Y. Ando, A. N. Lavrov, S. Komiya, K. Segawa, and X. F. Sun, Phys. Rev. Lett. **87**, 017001 (2001).

[25] C. Kusko, R. S. Markiewicz, M. Lindroos, and A. Bansil, Phys. Rev. B **66**, 140513R (2002).

[26] J. R. Schrieffer, X. G. Wen, and S. C. Zhang, Phys. Rev. B **39**, 11663 (1989).

[27] E. Kaneshita, M. Ichioka, and K. Machida, J. Phys. Soc. Jpn. **72**, 2441 (2003).

[28] L. P. Pryadko, S. A. Kivelson, V. J. Emery, Y. B. Bazaliy, and E. A. Demler, Phys. Rev. B **60**, 7541 (1999); O. Zachar, *ibid.* **65**, 174411 (2002).

[29] The distinct band structures may be manifested in the different transport properties of in-phase and antiphase stripes as seen by magnetoresistance measurements on lightly doped antiferromagnetic LSCO [Y. Ando, A. N. Lavrov, and S. Komiya, Phys. Rev. Lett. **90**, 247003 (2003)].

[30] N. Harima, J. Matsuno, A. Fujimori, Y. Onose, Y. Taguchi, and Y. Tokura, Phys. Rev. B **64**, 220507R (2001).

[31] See, for example, U. Löw, V. J. Emery, K. Fabricius, and S. A. Kivelson, Phys. Rev. Lett. **72**, 1918 (1994); A. H. Castro Neto, Phys. Rev. B **51**, 3254 (1995); S. R. White and D. J. Scalapino, Phys. Rev. Lett. **80**, 1272 (1998); E. Arrigoni, A. P. Harju, W. Hanke, B. Brendel, and S. A. Kivelson, Phys. Rev. B **65**, 134503 (2002).

[32] S. A. Kivelson (private communication).

[33] For an estimate of the long-range dielectric constant, see H.-B. Schüttler, C. Gröber, H. G. Evertz, and W. Hanke, cond-mat/9805133 (unpublished), and references therein.